



Elastic behavior of NiMgCuZn Ferrites in order to study the Phase Transitions

KEYWORDS

X-ray diffractions, SEM Morphologies, Elastic behavior, Ferrites, Microinductor applications.

N.VARALAXMI

Department of Physics, Kakatiya University, Warangal, Andhra Pradesh, INDIA.

K.V.SIVAKUMAR

Ceramic Composite Materials Laboratory, Department of Physics, Sri Krishnadevaraya University, S.V. Puram, Anantapur - 515 003, India

ABSTRACT This work investigates the elastic properties of NiMgCuZn ferrites. Ferrite samples were fabricated by means of the conventional double sintering technique. Magnesium nickel zinc and iron oxides were used as raw materials. The samples were sintered at 1250°C. The samples were then characterized by the X-ray diffraction (XRD), scanning electron microscopy (SEM) techniques. All these samples showed the formation of single-phase cubic spinel structure. The studies were carried out on the effect of temperature on the longitudinal modulus NiMgCuZnFe₂O₄ within temperature range 30°C to 360°C. A brief review of the important investigations carried out on the elastic behavior of different materials is listed out along a brief review of the different experimental techniques, employed to study the elastic behavior of solid materials is presented in this section with necessary theory. In the present investigation, the two composite piezoelectric resonator methods have been used. Results and discussions on the measurement of thermo elastic behavior of the present NiMgCuZnFe₂O₄ samples are discussed in all the series studied. Studies on these NiMgCuZn ferrites are under examination were developed for their possible application as core materials for microinductor applications.

1. Introduction:

The high potential applications of ferrites occupy an important place in the field of electronics; microwave and computer technologies have attracted the attention of many research workers in the field of materials science. They have advanced to a position of technological prominence in the last two decades. They are being extensively studied from the point of view of understanding their behaviour and applications. Recently there have been considerable advances in the understanding of the relationship between the microstructural characteristics and physical behaviour of ferrites. The increased knowledge has led to the development of desired microstructure in ferrites and also to the refinement of their manufacturing processes. The field of ceramic science and technology is therefore continuously growing in the light of these developments.

Measurements of elastic properties and acoustic losses are highly useful in the study of the phenomena such as phase transitions and relaxation processes in ferrites. This type of study leads to a knowledge of mechanical, magnetic and electrical losses in the ferrite materials and therefore, is of prime importance in their understanding from the point of view of their technological applications. These studies are also useful in the development of new compositions. In spite of the importance of such measurements not much work has been done on the experimental side excepting a few cases.

2. Brief Review of the work carried out on the Elastic behavior of ferrites:

Weil [1] was the first person to study the elastic behaviour of nickel and zinc ferrites. Using resonance method of magnetostriction, he studied the variation of Young's modulus in these ferrites having different densities and reported that the modulus increases with increasing density. By exciting extensional and torsional vibrations, van der Burgt [2] studied the elastic behaviour of Ni-Cu-Co ferrites. Fine and Kenney [3] using piezo-magnetic and piezo-electric methods, observed for the first time a low tem-

perature ordering transformation (95 K) in magnetite which was the source of large non-elastic effects. They attributed these non-elastic effects to stress induced ordering of Fe²⁺ and Fe³⁺ among octahedral sites in the lattice. The single crystal elastic constants of cobalt and cobalt-zinc ferrite at 30 °C were determined by Mc Skimin et.al., [4] using the phase comparison technique. In nickel-iron ferrites, Fine and Kenney [5], observed an acoustic relaxation effect occurring at 40 K. They attributed this to stress induced changes in the distribution of Fe²⁺ and Fe³⁺ ions in the lattice, involving electron diffusion. They estimated the activation energy necessary for this process to take place as 0.026 eV per electron jump.

Gibbons [6] studied systematically acoustic relaxations in ferrite single crystals. By employing composite oscillator method, he studied the elastic properties and internal friction of magnetite, nickel ferrite, manganese ferrite and manganese-zinc ferrite in the temperature range 4.2-350 K. He found, from the acoustic wave attenuation measurements, the existence of two types of stress-induced relaxations and a transformation. A loss mechanism due to stress induced electron migration of the type Fe³⁺ + e ↔ Fe²⁺, with an activation energy of 0.03 eV per electron jump appears to be common to all ferrites, containing divalent and trivalent ferrous ions on the octahedral sites.

Van der Burgt [7] found that the substitution of small cobalt content in nickel and nickel-zinc ferrites led to temperature independent permeability and elasticity in the latter. As a result, these ferrites possess a high figure of merit, suitable to be used in the construction of electrical and electromechanical filters. Anomalies in Young's modulus and damping capacity were observed in ferrite-chromites of lithium [8] which were attributed to ferrite becoming a compensated antiferromagnetic. Kimura and Kashihabara [9] measured the longitudinal and torsional velocities in nickel-zinc ferrites at 5 MHz using two crystal total internal reflection method. The dependence of elastic moduli on composition and firing conditions were discussed by them.

The Young's modulus as a function of magnetic field strength and frequency was studied in nickel ferrite by Kuznetsov [10]. He observed an anomaly in the Young's modulus at a frequency of 72 kHz. Kuznetsov [11] also found that the field dependence of ΔE and internal friction in nickel and nickel-zinc ferrites showed that Young's modulus passes through a maximum at a field corresponding to maximum permeability of the specimen.

Novikov et al., [12] determined Young's modulus of two mixed lithium ferrites by a resonance method in the temperature range 0-250 °C. A thermodynamic explanation was proposed by Belov [13] for the anomaly observed in the temperature dependence of Young's modulus in the thulium ortho-ferrite. In polycrystalline nickel-zinc ferrites Terstegge [14] studied the dependence of ΔE and mechanical Q factor on magnetic polarization and frequency. Haudek and Linke [15] excited longitudinal vibrations in toroids of manganese ferrite and manganese-zinc ferrites and studied ΔE -effect in the temperature range -150 to 200 °C. They considered that a zero passage of crystal anisotropy $K_i(T)$ is responsible for the observed anomaly in the ΔE versus T curves in manganese-zinc ferrites.

Using composite oscillator technique Seshagiri Rao et al., [16] determined the elastic constants of magnesium, cobalt, nickel and zinc ferrites at room temperature and mixed (Ni-Zn) Fe_2O_4 in the temperature range from 187 to 720 K [17-18] and mixed (Co-Zn) Fe_2O_4 [19-20] in the temperature range of 100 to 700 K. From a study of the temperature dependence of elastic moduli of these ferrites, Seshagiri Rao and Revathi [21] found that temperature dependence of elastic moduli follow Wachtman's equations [22]. Thermoelastic and magnetoelastic behaviour of $Co_{0.027}Mn_{0.02}Fe_2O_4$ has been studied by Kaczowski [23]. Reddy and Reddy [24] have studied thermoelastic behaviour of barium ferrite, $Mn_{0.58}Zn_{0.42}Fe_2O_4$, $Ni_{0.5}Zn_{0.5}Fe_2O_4$ and $Ni_{0.36}Zn_{0.64}Fe_2O_4$ in the temperature range 80-300 K employing composite oscillator technique.

The elastic behaviour of lithium-titanium mixed ferrites and mixed manganese-magnesium ferrites have been studied by Reddy et al., [25-26], Tanaka [27] studied the Young's modulus, shear modulus and bending strength of polycrystalline Mn-Zn ferrites with increasing Fe_2O_3 and decreasing oxygen content. Murthy et al., [20, 28-31] studied the magnetoelastic behaviour of mixed ferrites of Ni-Zn, Co-Zn, Mg-Mn and Li-Ni and observed the ΔE -effect. The authors have explained the ΔE -effect on the basis of domain rotation against uniaxial strain anisotropy and movement of 90° boundary walls. Murthy and Rao [31] studied the temperature dependence of Young's modulus and rigidity modulus behaviour of polycrystalline Li-Ni ferrites and they found that Y versus T and G versus T followed the Wachtman's relation [22].

Kawai and Ogawa [32] studied the changes of Young's moduli with magnetization (ΔE -effect) in (100), (110) and (111) directions of single crystal $Mn_{0.82}Fe_{2.18}O_4$ in the temperature range 150-300 K. Gendelev et al., [33] have grown the single crystal of $Mn_{0.62}Zn_{0.34}Fe_{2.4}O_4$ by Verneuil method and studied the elastic constants C_{11} , C_{12} and C_{44} . Komalamba et al., [34] studied the longitudinal modulus versus temperature from 300 to 630 K at zero magnetic field and at a magnetic field of 200 Oe for various samples of $Mn_yZn_{1-y}Fe_2O_4$. Belov et al., [35] studied the elastic and magnetoelastic behaviour of Erbium ortho ferrite. Ryabinkin and Kapitonov [36] have studied the elastic behaviour of Li-ferrite. Hoffmann [37] studied the magnetic,

magnetostrictive and elastic properties of Mg-Ni ferrites and found that nickel ferrite is superior to Mg-Ni ferrites as far as the magnetic and magnetostrictive properties are concerned. Marx [38] developed a three-part composite oscillator method in which he used two quartz rods, one as a driver and the other as a gauge, cemented to the specimen on either side of it. This method was widely used to calculate the acoustic damping of the specimen by many works.

Reddy studied the ΔE -effect in the case of $Mn_{0.58}Zn_{0.42}Fe_2O_4$ in the temperature range 80-300 K. Using Atomic Force Acoustic Microscopy, the Young's modulus of two thin films of nano crystalline ferrites with spinel structures has been measured as a function of oxidation temperature on a nano scale by Kester et al., [39]. Measurements of the elastic tensor elements and magnetostriction constants in the temperature range of 100 to 300 K were carried out in $Mn_xFe_{3-x}O_4$ and the elastic anisotropy constant K_1 coefficients B_1 and B_2 were deduced by Kawai et al., [40]. Effect of sintering temperature on elastic behaviour of mixed Li-Cd ferrites sintered at 1250 °C and 1300 °C was studied at room temperature by Ultrasonic-pulse transmission technique by Ravinder [41].

Elastic behaviour of manganese substituted lithium ferrites at room temperature was studied by the ultrasonic-pulse transmission technique at 1 MHz by Ravinder et al., [42]. Elastic behaviour of lithium-cobalt mixed ferrites has been investigated as a function of composition by Venudhar and Satyamohan [43]. An elastic behaviour in a single crystal of Mn ferrite ($Mn_{0.82}Fe_{2.18}O_4$) was studied at temperatures between 280 and 730 K by longitudinal vibrations of 125 kHz by Kawai and Ogawa [44].

Effect of temperature on the elastic and anelastic behaviour of magneto-ferroelectric composites $Ba_{0.8}Pb_{0.2}TiO_3 + Ni_{0.93}Co_{0.02}Mn_{0.05}Fe_{1.95}O_{4.8}$ in the ferro electric rich region in the temperature range 300 to 600 K was carried out by Ramamanohar Reddy et al., [45]. A simple system using one crystal composite oscillator for internal friction and modulus measurements was developed by Schwarz [46]. A study of elastic behaviour and internal friction of aluminium substituted magnesium-copper ferrites have been carried at room temperature by ultrasonic pulse transmission technique by Venugopal Reddy et al., [47]. Reddy and Reddy [48] have determined the Young's modulus and rigidity modulus of polycrystalline $Mn_{0.58}Zn_{0.42}Fe_2O_4$ using the composite oscillator technique. Gibbons [49] has studied the temperature variation of ΔE in the single crystal $Mn_{0.14}Zn_{0.86}Fe_2O_4$ along <110> in the low temperature range. A linear dependence of longitudinal velocity (v_l) on density (ρ) for rocks having the same mean atomic weight (M/P), where P is the number of atoms in the structural unit and M is the molecular weight was first suggested by Birch [50-51]. Simmons [52-53] has confirmed this evidence and showed that the shear velocity (v_s) also varies linearly with density. Following this work, Anderson [54] has demonstrated that (v_l/ρ) and (v_s/ρ) are constant for large number of oxide minerals having the same mean atomic weight.

Elastic properties of mixed Li-Cu ferrites as a function of composition at room temperature were investigated by Ravinder and Vijaya Bhaskar Reddy [55]. Ravinder and Ravi Kumar [56] studied the elastic behaviour of rare earth substituted Mn-Zn ferrites. Ravinder [57] also studied the elastic behaviour of lithium ferrites. Elastic behaviour of Cu-Zn and composition dependence of elastic behaviour

of mixed manganese-zinc ferrites were investigated by Ravinder et.al., [58-59].

Elastic behaviour of Zn substituted LiMg and LiMgTi ferrites were carried out by Nitendar Kumar et.al., [60]. Abd El-Ati and Tawak [61] studied the Young's modulus of $Ni_{0.65}Zn_{0.35}Cu_xFe_{2-x}O_4$ where $x = 0.0, 0.1, 0.2, 0.3, 0.4$ and 0.5 , and observed that Young's modulus decreased with increasing Cu content. This is due to the fact that Cu^{2+} ions entered the lattice substitutionally for Fe^{3+} ions at the octahedral sites, creating lattice vacancies gave rise to lattice strain.

From the above review, the author notices that the experimental work carried out on the thermoelastic behaviour of NiMgCuZn ferrites is scanty. In view of this, the author has studied the effect of temperature on the longitudinal modulus of nickel magnesium copper zinc ferrites and results are presented in this chapter. It may be mentioned here that these NiMgCuZn ferrites are under examination were developed for their possible application as core materials for microinductor applications.

2.1. Elastic wave propagation in Isotropic solids:

In a solid body, stress can be resolved into three extensional and three shear components. Similarly strain produced in a body can also be resolved into six components. According to Hooke's law, when strain is small, each component of stress can be expressed as a linear combination of the strain components and vice versa. There may be large number of proportionality constants for most anisotropic materials. Triclinic system has got 21 proportionality or elastic constants.

For an isotropic solid, the elastic moduli are not functions of direction. Applying the symmetry conditions, one finds that the independent elastic constants are two only for an isotropic body.

For an anisotropic body, the six stress-strain equations are given by

$$\begin{aligned}
 T_1 &= (\lambda + 2\mu) S_1 + \lambda(S_2 + S_3) = \lambda \Delta + 2\mu S_1 \\
 T_2 &= (\lambda + 2\mu) S_2 + \lambda(S_1 + S_3) = \lambda \Delta + 2\mu S_2 \\
 T_3 &= (\lambda + 2\mu) S_3 + \lambda(S_1 + S_2) = \lambda \Delta + 2\mu S_3 \\
 T_4 &= \mu S_4 \\
 T_5 &= \mu S_5 \\
 T_6 &= \mu S_6 \quad \dots \quad (1)
 \end{aligned}$$

where

$$\Delta = S_1 + S_2 + S_3 \quad \dots \quad (2)$$

T_i 's are six stresses

S_i 's are six strains

λ and μ are the two Lamé' constants.

The other three constants of fundamental importance are Young's modulus (E), bulk modulus (K) and the Poisson's ratio (σ). Young's modulus can be expressed as the ratio of longitudinal stress to longitudinal strain in a bar, when extensional stress is applied along one axis. When the

extensional stress is applied along Z-axis,

$$T_1 = T_2 = 0.$$

Solving for the ratio of T_3 to S_3 by eliminating S_1 and S_2 from Eqn. (1) Young's modulus E can be obtained.

Therefore,

$$E = \frac{T_3}{S_3} = \frac{\mu(3\lambda + 2\mu)}{(\lambda + \mu)} \quad \dots \quad (3)$$

Instead, if we take the ratio between S_1 and S_3 Poisson's ratio is obtained.

$$\sigma = -\frac{S_1}{S_3} \quad \dots \quad (4)$$

σ can be expressed as

$$\sigma = \frac{\lambda}{(2\lambda + \mu)} \quad \dots \quad (5)$$

By setting $T_1 = T_2 = T_3 = -p$ and solving for Δ , the change in volume, we get

$$\Delta = \frac{-3p}{(3\lambda + 2\mu)} \quad \dots \quad (6)$$

The bulk modulus K is defined as the ratio of hydrostatic pressure p to the relative change in volume of the material.

Therefore,

$$\frac{p}{\Delta} = \frac{3\lambda + 2\mu}{3} + \lambda + \frac{2}{3}\mu = K \quad \dots \quad (7)$$

Applying Newton's second law of motion, the equations of motion for waves in an unbounded medium can be derived. If an elementary cube of volume $dx \, dy \, dz$ is considered, the equations derived from Newton's laws of motion are

$$\rho \frac{d^2 u_i}{dt^2} \, dx \, dy \, dz = F_i \, (i = 1, 2, 3) \quad \dots \quad (8)$$

where u_i are the displacements viz., u, v and w along the 1-, 2- and 3- axis respectively and ρ is the density of the solid. The force components F_i in the three directions are determined by the rate of change of stress along the edges of the unit volume and can be written as

$$F_i \frac{\partial T_j}{\partial X_j} \, dx \, dy \, dz \quad \dots \quad (9)$$

Eqn. (8) can be written as

$$\rho \frac{\partial^2 u_i}{\partial t^2} \, dx \, dy \, dz = \frac{\partial T_j}{\partial X_j} \, dx \, dy \, dz \quad \dots \quad (10)$$

But each stress component is related to its corresponding strain component through the elastic constant C_{ijkl} , and hence

$$\frac{\partial^2 u_i}{\partial t^2} = \frac{\partial C_{ijkl} S_k}{\partial X_j} \quad \dots \quad (11)$$

For an isotropic solid, the above equation reduces to the three well known equations as given below.

$$\begin{aligned}
 \rho \frac{\partial^2 u}{\partial t^2} &= \frac{\partial}{\partial x} (\lambda \Delta + 2\mu S_1) + \frac{\partial}{\partial y} (\mu S_6) + \frac{\partial}{\partial z} (\mu S_2) \\
 \rho \frac{\partial^2 v}{\partial t^2} &= \frac{\partial}{\partial x} (\mu S_6) + \frac{\partial}{\partial y} (\lambda \Delta + 2\mu S_2) + \frac{\partial}{\partial z} (\mu S_4) \\
 \rho \frac{\partial^2 w}{\partial t^2} &= \frac{\partial}{\partial x} (\mu S_5) + \frac{\partial}{\partial y} (\mu S_4) + \frac{\partial}{\partial z} (\lambda \Delta + 2\mu S_3) \quad \dots \quad (12)
 \end{aligned}$$

where $\Delta = S_1 + S_2 + S_3$

According to Christoffel, the equation of motion for the Eqn. (12) could be written in terms of u, v, w and s (where $s = lx + my + nz$ and l, m, n are the direction cosines of the normal to the plane wave) by introducing a series of moduli λ_{11} to λ_{33} which are functions of the Lamé constants and the direction cosines l, m, n .

Hence, Eqn. (12) assumes the form

$$\begin{aligned} \rho \frac{\partial^2 u}{\partial t^2} &= \lambda_{11} \frac{\partial^2 u}{\partial s^2} + \lambda_{12} \frac{\partial^2 v}{\partial s^2} + \lambda_{13} \frac{\partial^2 w}{\partial s^2} \\ \rho \frac{\partial^2 v}{\partial t^2} &= \lambda_{12} \frac{\partial^2 u}{\partial s^2} + \lambda_{22} \frac{\partial^2 v}{\partial s^2} + \lambda_{23} \frac{\partial^2 w}{\partial s^2} \\ \rho \frac{\partial^2 w}{\partial t^2} &= \lambda_{13} \frac{\partial^2 u}{\partial s^2} + \lambda_{23} \frac{\partial^2 v}{\partial s^2} + \lambda_{33} \frac{\partial^2 w}{\partial s^2} \dots (13) \end{aligned}$$

where

$$\begin{aligned} \lambda_{11} &= l^2 (\lambda + \mu) + \mu \\ \lambda_{12} &= lm (\lambda + \mu) \\ \lambda_{13} &= nl (\lambda + \mu) \\ \lambda_{23} &= mn (\lambda + \mu) \\ \lambda_{22} &= m^2 (\lambda + \mu) + \mu \\ \lambda_{33} &= n^2 (\lambda + \mu) + \mu \dots (14) \end{aligned}$$

For the isotropic medium, the solution for Eqn. (14) indicates the propagation of three waves. The particle motion in a direction perpendicular to the direction of propagation is possible only in certain special cases. However, the three velocities satisfy the equation

$$\begin{vmatrix} (\lambda_{11} - \rho v^2) & \lambda_{12} & \lambda_{13} \\ \lambda_{12} & (\lambda_{22} - \rho v^2) & \lambda_{23} \\ \lambda_{13} & \lambda_{23} & (\lambda_{33} - \rho v^2) \end{vmatrix} = 0 \dots (15)$$

Evaluating the determinant and using the relation for the direction cosines

$$l^2 + m^2 + n^2 = 1 \dots (16)$$

Eqn. (15) becomes

$$(\lambda + 2\mu - \rho v^2) (\mu - \rho v^2)^2 = 0 \dots (17)$$

Thus, independent of the orientation employed, there is one wave with velocity v_1 in which the particle vibration is in the direction of propagation (a longitudinal wave), and two waves with velocity v_s , for which the direction of particle vibration is normal to the direction of wave propagation (shear wave)

$$v_1 = \left[\frac{\lambda + 2\mu}{\rho} \right]^{1/2}; \quad v_s = [\mu/\rho]^{1/2} = [G/\rho]^{1/2} \dots (18)$$

where v_1 and v_s represent the longitudinal and (shear wave) velocities respectively.

Thus, using Eqns. (3), (7) and (18), we can evaluate the Young's modulus (E), bulk modulus (K), rigidity modulus (G) and Lamé constants λ and μ .

2.2. Brief review of experimental methods employed for measurements of elastic constants of solids:

A brief review of the different experimental techniques employed to study the elastic behaviour of solid materials is presented in this section.

The methods can be broadly classified into four categories, they are - (i) static methods, (ii) dynamic methods, (iii) X-ray methods and (iv) ultrasonic methods. Static methods give isothermal moduli whereas the dynamic methods based on resonance techniques give usually the adiabatic moduli.

(a) Static methods

The early methods used were static ones consisting of bending and twisting of crystal plates and crystal bars under investigation, to determine the elastic constants of the crystals. In the classical experiments, Voigt [62] has made use of the above principles. Refinements in these experiments were later on introduced by Tutton [63] incorporating interferometric techniques for the measurement of strains. A follow up of the improved static methods was carried out by Bridgman [64], Mandell [65], Hanson [66], Hinz [67], Swift and Tyndall [68] and others. The chief drawback of these static methods is that they are not suitable for the determination of the elastic constants of solids, when samples are available in small sizes. Hence a number of dynamic resonance methods have been developed for the measurement of the elastic moduli of the solids.

(b) Dynamic methods

In dynamic methods, generally the specimen is set into vibration employing an electrostatic or electromagnetic or magnetostrictive or piezoelectric transducer. Direct application of vibration methods to crystals have been made by Wright [69], Davies [70], Goens [71], Mason [72] and Hunter and Siegel [73].

Vibrational studies of plates have also been used to measure elastic constants, particularly for piezoelectric crystals. Atanasoff and Hart [74] in their method used crystals directly in the electrical circuits. This method was employed by Bhagavantam and Suryanarayana [75] to determine the elastic constants of tourmaline and zinc blende crystals. This method has got a very restricted application and the results obtained are to be corrected for the influence of piezoelectric effects.

To study the elastic properties of rock specimens, Ide [76] used the electrostatic method of exciting the specimen into vibrations. To determine the velocity of extensional waves in metals such as lead, tin, aluminium and cadmium up to their melting points, Bordoni [77] adopted this method.

For setting rods into torsional and longitudinal vibrations, Fine [78] and Wegel and Walther [79] described a method using a magnetic device. Forster [80] and Forster and Koster [81], developed resonance methods where in flexural vibrations are excited in the rods by an electromagnetic drive. Spinner [82] also adopted this method to excite torsional vibrations in isotropic bars. Several other workers employed this method to study the elastic properties of refractory oxides. Bradfield [83] reviewed the use of magne-

tostrictive transducers to excite the longitudinal and shear vibrations of rock samples. Van der Burgt [84] determined the dynamic constants of nickel and nickel-zinc ferrites using a magnetostrictive method.

(c) X-ray methods

X-ray method of determining the elastic constants by measuring the intensity of the monochromatic X-rays, which in turn interact with the lattice vibrations, has been used by Curien [85], Jacobsen [86] and Johnson [87] to determine the force constants of iron, copper and zinc. Gunther [88] used X-ray diffraction technique to measure the elastic constants of aluminum. Wooster and Ramachandran's [89] approach depends on the coherently diffracted X-radiation which is scattered by the interaction with the thermal waves of the lattice. In these methods, the absolute accuracy that is attainable is poor compared to that achieved in dynamic methods.

(d) Ultrasonic methods

Bergmann and Schaefer [90] were the earliest workers to make use of the piezoelectric phenomenon of quartz for a study of crystal elasticity. In their method a fair sized, well polished and transparent cube of the material is set into vibration by a quartz crystal. Due to couplings at the boundaries and reflections of the waves, both longitudinal and torsional, a sort of three-dimensional grating will be set up in the cube. If light from a circular aperture traverses such a medium, characteristic diffraction pattern results. The elastic constants are determined from the dimensions of the diffraction pattern, a constant that is characteristic of the experimental set up and the operating frequency. This method is obviously suitable for transparent solids. But, in a later development [91], the method is applied to opaque bodies also. Here the light is reflected from the surface of the vibrating specimen, the difficulty with this method lies in that to get fairly intense diffraction patterns, one has to apply a large amount of power to the crystal which involved temperature fluctuations in the specimen. This makes it particularly unsuitable for applying the method to a study of the temperature dependence of elastic constants. Further the accuracy attainable is often only of the order of 5 per cent or higher.

Hiedemann and his co-workers [92] utilizing the phenomenon of diffraction of light by ultrasonic waves developed a technique for determining the elastic constants of isotropic solids. Later on, this method was extended to crystals also by Bhagavantam and Ramachandra Rao [93]. For successful application of this method, one has to employ well polished crystals at high frequencies.

Some of the defects pointed in the above methods have been eliminated in the wedge method developed by Bhagavantam and Bhimasenachar [94]. It concerns with the study of the vibrational modes of non-piezoelectric crystal plates. Also, this method has the obvious advantage of being applicable to opaque media. The specimen in the form of a plate is excited by a quartz wedge driven by an alternating current of variable frequency there by providing a continuous supersonic spectrum. The specimen is in contact with a liquid through which a light beam is passed. As the exciting frequency is varied, an appropriate portion of the wedge resonates and produces an ultrasonic beam of the same frequency. These resonant frequencies of the specimen are detected by the maximum in the diffraction effects on the light produced by the ultrasonic grating in the liquid. The transmission frequencies thus measured have to be sorted out and assigned to their

appropriate modes. A sufficient number of such determinations permit one to calculate the complete set of the elastic constants. This method has an advantage because one can use every small specimen for determining elastic constants. This fact facilitated the determinations of the elastic constants of diamond [95]. In these experiments, the frequency range employed is from 0.5 to 10 MHz and the accuracy realizable is about five per cent.

A major drawback of this method is that the specimen under investigation comes into contact with liquid. This method cannot be applied to substances which have a tendency to absorb liquid. The same defect makes it unsuitable for the temperature work also.

The advent of radar techniques has made available, in recent years, electronic methods for the timing of short high frequency pulses of ultrasonic power. The method has been employed to study the elastic constants of the solids by Huntington [96], Arenberg [97], McSkimin [98], Bacon and Smith [99] and Musgrave [100]. A quartz crystal is cemented to one of the two plane parallel faces of the specimen. A pulse of the order of microsecond duration is generated and transmitted through the specimen. On reflection at the opposite surface, it returns and when it arrives back at the quartz transducer, it gives rise to an electrical signal or echo. It is possible to observe a whole sequence of such echoes and this makes possible the measurement of transit time more accurately. X-cut quartz and Y-cut quartz transducers having resonant frequencies at 10 MHz are usually employed to excite longitudinal and transverse waves respectively. The pulse technique has proved valuable in the study of the influence of temperature [101-103] and pressure [104-106] on the elastic constants of crystals. Accuracy better than one percent is easily achievable in this method. Interferometry has been combined with pulse technique to attain higher precision in the velocity measurements with small specimens [107-109]. The specimens are mounted on the ends of fused quartz rods so the initial pulse. The pulse length can be extended until several pulses overlap. The frequency is varied until the condition for constructive interference is indicated by a clear step pattern in the overlapping echoes. In obtaining acoustic velocity from differences between these resonant frequencies the phase shifts introduced due to reflections at the boundaries of the specimen have to be taken into account.

But all the ultrasonic methods, with the exception of pulse technique, have one defect or the other, because of which they are not suitable for the study of the elastic constants as a function of temperature.

All these defects are taken care of in the composite piezoelectric resonator technique developed originally by Balamuth [110] and Rose [111]. In this technique, a small sample in the form of a rod with square or circular cross-section is cemented to a piezoelectric crystal. Determination of the resonant frequencies of the quartz and the composite system makes it possible to calculate the natural frequency of the specimen and thereby its elastic constants.

In the present work in order to study the temperature variation of longitudinal modulus (L) of nickel magnesium copper and zinc ferrites the author has developed a two component piezoelectric resonator technique, the details of which are presented in the next section. This work has been under taken to study the longitudinal modulus of

these ferrites to test their suitability as core materials used for micro inductor applications.

2.3. Composite oscillator technique:

In the present investigation the composite piezoelectric oscillator technique originally developed by Balamuth [110] and Rose [111] with a few modifications has been set up in this laboratory.

(a) Theory of the composite piezoelectric oscillator method

Composite resonator technique is based on the principle of determination of the natural frequency of a loaded bar executing either longitudinal or torsional oscillations. A precision electrical oscillator is used to excite an X-cut quartz transducer of suitable length and resonance is detected by observing the amplitude of the resulting current. The system attains a state of forced vibrations owing to the harmonically varying piezoelectric stress in the quartz which accompanies the electric field between the electrodes. The frequency of the forced vibration is the same as that of the applied potential difference. Thus the natural frequency of the quartz bar is known. The test specimen of identical cross-section having a natural frequency slightly different from that of the quartz transducer is cemented to one end of the quartz bar with a suitable adhesive and the fundamental resonant frequency of the composite system is measured in the same manner. The frequency of the specimen bar is then deduced from which the appropriate elastic constant is calculated using the length and density of the specimen. Similarly for exciting torsional oscillations, a Y-cut quartz rod with four electrodes is used. The impedance of the quartz crystal and the composite system undergoes a marked reduction at their respective resonant frequencies. Hence this method needs an expression system and the quartz with their respective impedances. The theoretical treatment as given by Balamuth [110] is briefly outlined here.

According to Van Dyke [112] the charge necessary to establish a potential difference (V) between the electrodes of the transducer can be separated into two parts (i) the ordinary capacitive part equal to C' where C' is the inter-electrode capacitance and (ii) that required to neutralize the piezoelectric charge produced by the vibrational strain in the quartz and proportional to the space average value of its strain given by k'ε_{av}.

The net charge Q is given by

$$Q = C'V - k'\epsilon S_{av} \dots (19)$$

where ε, k' and S_{av} represent appropriate piezoelectric coefficient, geometric constant and average strain respectively.

The current I flowing through the oscillator is given by

$$I = C' \frac{dV}{dt} - k' \epsilon \frac{dS_{av}}{dt} \dots (20)$$

The piezoelectric stress in the quartz cylinder is represented by harmonically varying surface tractions over its end faces. The equation of motion of the oscillator is of the form.

$$\rho \frac{\partial^2 u}{\partial t^2} = P \left\{ 1 + T \frac{\partial}{\partial t} \left(\frac{\partial^2 u}{\partial x^2} \right) \right\} \dots (21)$$

where u, ρ, P and T represent particle displacement, density, the appropriate elastic modulus and dissipation coef-

ficient respectively.

The particle displacement u in each medium is given by

$$u = [A \exp (\alpha + j\beta) x + B \exp - (\alpha + j\beta) x] e^{j\omega t} \dots (22)$$

where

$$\omega = 2 \pi f$$

$$\alpha = \omega (\rho / P)^{1/2}$$

$$\beta = \frac{\omega T}{2}$$

Since T is sufficiently small ω² T² << 1. The four amplitude coefficients (A and B of each medium) are evaluated by means of the four simultaneous equations which express the continuity of stress and displacement at the interface and of stress at the end faced of the oscillator respectively. The strain average S_{av} is calculated from the expression for u in the quartz and the electrical impedance of the oscillator from Eq. (20). The electrical impedance Z can be written as

$$1/Z = j \omega C' + 1/Z_m \dots (23)$$

In the vicinity of the resonance, the form of expression for Z_m is the same as that for the electrical impedance of a series resonant circuit. It follows that, near resonance, a composite resonator is electrical equivalent to a series electrical network of impedance Z_m shunted by a capacitance C'.

If Z_m is written in the form

$$Z_m = R + jx \dots (24)$$

Then for a two part oscillator (quartz transducer and specimen)

$$R = (k \omega / D) \left[\left(\frac{M_1 Z_1}{Y_1} \right) (\sec^2 Y_1 - p_1) + \left(\frac{M_2 Z_2}{Y_2} \right) (\sec^2 Y_2 - p_2) \right] \dots (25)$$

and

$$X = \left(\frac{k \omega}{D} \right) (M_1 p_1 + M_2 p_2) \dots (26)$$

Where

$$D = (1 - \sec^2 Y_1) \left[\left(1 - \frac{P_2 Y_2^2}{Y_1} \right) (M_1 P_1) \right]$$

k = a constant

M_i = mass of the cylinder (i = 1, 2)

Z_i = α_i L_i

L_i = length of the cylinder (i = 1, 2)

$$Y_i = \frac{\pi f}{f_i}$$

$$f_i = (1/2L) (P/P)^{1/2}$$

$$p_i = (\tan Y_i) / Y_i$$

where, f is frequency of the composite system and subscript 1 and 2 refer to specimen and quartz respectively. The resonant frequencies are those at which the reactive

part vanishes, i.e. $M_1 p_1 + M_2 p_2 = 0$

$$M_1 = \frac{\tan(\pi f / f_1)}{(\pi f / f_1)} + M_2 \frac{\tan(\pi f / f_2)}{\pi f / f_2} = 0 \quad \dots (27)$$

when $M_1 = 0$, Eqn. (27) describes the behaviour of quartz alone. Frequency of the specimen f_1 can be computed from the Eqn. (27) by knowing f and f_2 .

An approximate solution for Eqn. (27) may be given as

$$f_1 = f + (M_2/M_1) (f-f_2) \quad \dots (28)$$

Eqn. (28) can be used only if f , f_1 and f_2 differ by about 10%.

This condition is always satisfied throughout the present investigation.

The natural frequencies of the specimen for longitudinal vibrations may be written as

$$f_1 = 1/2L (E/\rho)^{1/2} \left[1 - \frac{\pi^2 \sigma^2 \theta}{2AL^2} \right] \quad \dots (29)$$

where E , L , σ and A represents the Young's modulus, length, Poisson's ratio and area of cross-section of the sample, and

$$\theta = \frac{M(a^2 + b^2)}{12}$$

is the moment of inertia of rectangular parallelepiped (specimen) about the cylinder axis. a and b represent the thickness and breadth of the sample respectively. M represents the mass of the specimen.

The equation (29) can be written as

$$f_1 = 1/2L (E/\rho)^{1/2} \left[1 - \frac{\pi^2 \sigma^2 (a^2 + b^2) M}{24L^2 ab} \right] \quad \dots (30)$$

The resonant frequency of the torsional vibrations f_s is related to the dimensions of the specimen by the formula

$$f_s = 1/2L (G/\rho)^{1/2} \quad \dots (31)$$

where G represents the rigidity modulus.

Since the value of σ is generally small, it can be neglected for calculating Young's modulus (E) from Eqn. (31). However, σ may be computed with sufficient accuracy with approximate values of elastic constants obtained when the term is set equal to zero and this value of σ is used to obtain the correction. Using this value of σ the final value of E is obtained from Eqn. (31).

(b) Description of the experimental setup

The block diagram of the composite oscillator technique employed to excite and detect the resonant vibrations of the piezoelectric oscillator is shown in Fig.1. Radio frequency output from the signal generator SG (designed and rigged up in this laboratory) is connected across a turned circuit which is loosely coupled to the output stage of the amplifier. The frequency of the signal generator is controlled in part by an incremental turning capacitor whose full scale represents 2 kHz in the range 80 to 200 kHz. The stability of the signal generator is better than 5 Hz. The actual frequency of the signal generator has been measured using Yamuna Digital Frequency Counter Model 626, capable of giving accuracy 1 in 10^6 .

To keep the voltage across the crystal constant, a regulated voltage is supplied to the amplifier. In this set up by changing the output from the signal generator the voltage across the crystal can be changed from 2 to 200 V.

The composite bar and the loading circuit form a parallel tuned circuit and so its impedance is maximum at resonance. A micro ammeter in series with the crystal diode IN34 is used as a detector to trace the response of the coupled circuit. The resonant frequency of the oscillator is indicated by a minimum deflection in the micro ammeter.

(c) Preparation of quartz crystals

X-cut quartz bars of square cross-section as shown in Fig.2 are used for exciting longitudinal vibrations in the specimen. The faces normal to the electric axis are silvered and supported by the crystal holder at its nodal points. The crystal holder contains two porcelain rods mounted on a porcelain base. Two phosphor bronze strips bent in the form shown in Fig.2 are fixed to the porcelain bars. Silver tips are attached to the phosphor bronze strips to form the electrodes for good contact with the crystal. The quartz bars used are 4mm square in cross-section.

The quartz selected for preparing X-cut the transducers should satisfy the following requirements.

- (i) The frequency versus temperature graph of the quartz should not be discontinuous.
- (ii) In preparing the quartz transducer sufficient care must be taken to avoid the harmonics of the low frequency flexural modes lying very close to the natural frequency from the mode of vibration to the other.

A set of quartz transducers were prepared from the natural quartz crystal free from the defects. Each specimen under investigation has to be tried with different quartz transducers so as to satisfy the condition that the frequency of the composite oscillator and that of quartz lie within 10%.

Basic data of the quartz transducer employed in the present investigation are given in the Table.1.

(d) Cementing

The composite oscillator is formed by cementing the quartz rod to the specimen of identical cross-section. For room temperature measurements, phenyl salicylate commonly known as "salol" is used as the bonding material. For the high temperature work, the adhesive that can be used consists of five parts of sodium metasilicate and one part of calcium carbonate. These chemicals should be thoroughly powdered to micron size and mixed with a drop or two of double distilled water so as to form a very fine paste. A thin layer of this paste is used for bonding the transducer with the specimen. The composite system so formed is to be kept under pressure at least for about 24 hours at room temperature before it is put into use at high temperatures. The following precautions are to be taken in the process of cementing.

- (i) A thin layer of adhesive is to be used. As pointed out by Balamuth [110], the effect of the cement is negligible on the frequency of the composite system provided the frequencies of the specimen and the composite system are within 5 to 10%. The condition is satisfied throughout the present investigation.
- (ii) There should not be any amount of cement left off adhering to the sides of the composite system. Such excess if left produces loading effects in the composite oscillator.

(e) Temperature study

Using the two-part composite piezoelectric oscillator, longitudinal modulus was measured upto a temperature of $\approx 400^\circ\text{C}$ in the present investigation. An electric furnace which can go up to 450°C has been constructed and used in the present investigation. The electric furnace consists of a thick fused silica tube over which nichrome wire of sufficient length was wound at regular intervals non-inductively. To avoid loss of heat due to radiation, a thick lining of ceramic wool padding was given on the nichrome wire and kept in a cylindrical asbestos tube. The space between this silica tube and asbestos tube was filled with ceramic wool. The cylindrical tube was closed with porcelain lid consisting of the crystal holder arrangement. The temperature of the furnace was raised by passing current through the heating element by a variac. The temperature of the furnace could be controller to any desired value with an accuracy of $\pm 0.2\text{ K}$ using CPC (Consolidated Process and Controls Pvt Ltd., Bangalore) temperature controller-indicator Digit Temp 102. A cromel-alumel thermocouple which acts as both temperature sensing and controlling element was inserted into the furnace through the hole provided for it without touching the sample but situated very close to it. The composite oscillator was suspended inside the furnace such that its axis exactly coincides with the axis of the cylindrical furnace.

(f). Accuracy of the method

The chief source of error in this method of measurement is non-uniformity of the cross-section in the specimens. Such non-uniformity produces a small shift parallel to itself of the entire velocity versus temperature curve. The estimated uncertainty in the absolute measured velocities is 0.5 to 1%. However, greater accuracy can be achieved in making relative measurements of the velocities rather than their absolute values. These factors have been taken into account while fitting the curves to observed points.

2.4. Thermo elastic behavior of sodium chloride comparison with the literature data:

To test the reliability of the composite piezoelectric oscillator technique developed in the present investigation, measurement of S_{11} as a function of temperature has been made on single crystal specimens of sodium chloride grown from Bridgman technique has been used.

The values of elastic compliances S_{11} at different temperatures obtained in the present work are presented in the Table.2. The present data is compared with the values obtained by Hunter and Siegel [73].

An examination of the data presented in the Table.2 shows that there is a good agreement between the compliance values of present work and that of literature. This establishes the reliability of the composite-oscillator technique developed in the present investigation.

3. Experimental methods:

In the present investigation, the three series of NiMgCuZn ferrites were synthesized

Series - I. $\text{Ni}_x\text{Mg}_{0.6-x}\text{Cu}_{0.1}\text{Zn}_{0.3}\text{Fe}_2\text{O}_4$ where 'x' varies from 0.0, 0.1, 0.2 and 0.3
Series - II. $\text{Ni}_{0.3}\text{Mg}_x\text{Cu}_{0.1}\text{Zn}_{0.6-x}\text{Fe}_2\text{O}_4$, where 'x' varies from 0.1, 0.2 and 0.3
Series - III. $\text{Ni}_{0.35}\text{Mg}_x\text{Cu}_{0.05}\text{Zn}_{0.6-x}\text{Fe}_2\text{O}_4$ where 'x' varies from 0.0, 0.1 and 0.2

In the present investigation, the nickel-magnesium-copper-zinc ferrites were prepared by employing conventional solid state reaction route by mixing analytical grade NiO,

MgO, CuO, ZnO and Fe_2O_3 in stoichiometric proportions. These oxides were mixed and ground together using agate mortar for 8 hours. This mixture was pressed into a cake and presintered at 800°C for 12 hours taking enough care to avoid the evaporation of zinc and is cooled to room temperature. The pre-sintered cake was crushed and was ground in agate mortar to obtain fine particle size. This powder was sieved to obtain uniform particle size.

These mixed powders were pressed with the help of the hydraulic press applying a pressure of 25 kN using a high carbon high chromium steel die into the required shape. The binder used in the present work is 2% polyvinyl alcohol, dissolved in the water. Occasionally stearic acid dissolved in the acetone was also used as lubricant to prevent sticking of powder to the walls of the die. Various desirable shapes like pellets, bars, cylinders and torroids depending on the requirement of the experimental technique, the green powders of the ferrites were pressed in suitable dies and they were loaded on a ceramic block containing 'V' shaped grooves to prevent bending of the samples during the final sintering process at high temperatures. After loading the ceramic block in to the furnace, the temperature of the furnace was raised to 110°C in a period of 1 hr and maintained at 110°C to remove the residual water content if any from the samples. Then the furnace temperature was raised to 800°C at the rate of $80^\circ\text{C}/\text{hr}$ and maintained there for one more hour for the burning of binder used in the samples. Bars of square cross section of $4 \times \text{mm} \times 4 \times \text{mm}$ and $2.05 \times \text{cm}$ were prepared in order to study the effect of temperature on internal friction loss and longitudinal modulus in these ferrites. Lastly, the final temperature of 1250°C was achieved at the rate of $100^\circ\text{C}/\text{hr}$. A soaking time of 3 hrs is maintained and later, the samples were cooled to room temperature at the rate of $80^\circ\text{C}/\text{hr}$. After cooling, the samples were removed from the furnace. Enough care was taken to avoid the evaporation of zinc during the sintering process.

4. Results:

X-ray diffraction patterns obtained in the present investigation for various ferrites are presented in Fig.3. An examination of these X-ray diffractograms shows that these ferrite samples reveal the formation of single phase cubic spinel structure.

The lattice parameter (a), the unit cell volume (V) and density (ρ) of all the samples are calculated. The lattice parameters in series I decrease with decreasing Mg^{2+} content, where as in series II and III the simultaneous increase and decrease of magnesium and zinc results in a nominal decrease of lattice parameters.

The typical scanning electron micrographs of a few ferrite samples are presented in Fig.4. An examination of these figures shows that there is no second phase formation.

5. Discussions:

Table.3 represents the longitudinal modulus data for different compositions of all the three series at room temperature. The temperature variation of longitudinal modulus data for series I is graphically shown in Fig.5. In the absence of any phase transition in most of the solids the velocity decreases with an increase in temperature, and hence the modulus also decreases with temperature.

According to Eyring and Kincoide [113-114] the sound wave travels with infinite velocity within the atom and with a

gas kinetic velocity in the void space between the atoms. Hence, the velocity in a close packed arrangement of atoms is more than in the loose packed arrangement of the same atoms. Due to the thermal expansion of the solid, the interatomic distance increases which in turn decreases the velocity and hence, the modulus. This behaviour is observed in all the samples near the Curie temperature marked by arrows. Fig.5 indicates that there is a systematic decrease of longitudinal modulus as a function of temperature. Also it can be seen in all that there is a sharp fall in modulus at a particular temperature which exactly coincides with the Curie temperature transition. Hence below T_c the ferrite samples are in ferrimagnetic phase and above T_c the sample show paramagnetic phase. The Curie temperature data and the temperatures corresponding to sharp falls in all the graphs are shown in Table.3 for comparison. Since the ferrites are ferrimagnetic solids as the temperature increases they transform from ferrimagnetic phase to paramagnetic at certain temperature called Curie temperature. Where they lose their domain structure and the magnetic dipoles become free. This is a phenomenon that is connected to the lattice, hence the longitudinal modulus shows a lattice instability at T_c , which is depicted by a sharp fall at T_c in longitudinal modulus versus temperature behaviour. Changes in the elastic moduli usually accompany changes of phase. This type of discontinuous behaviour in modulus was reported by Koster and Banger [115] in Hume-Rothery alloys. Young's modulus falls discontinuously, sometimes by a factor of two and the internal friction shows a sharp peak in the same region [116].

Since the elastic modulus is a lattice related property it clearly depicts the changes in the unit cell and hence shows phase transitions in an unambiguous way. As the nickel composition in this ferrite series increases the Curie temperature increases.

The temperature variation of longitudinal modulus data for this series II and series III is diagrammatically represented in Figs. 6 and 7. A glance at the figures indicates that the phase transition occurs at Curie temperature for all the compositions. One can see from the figures that there is a systematic decrease of longitudinal modulus as a function of temperature. As the magnesium content in the ferrite system increases the temperature corresponding to the abrupt fall in longitudinal modulus shifts to higher temperature side, a discontinuity is noticed in longitudinal modulus versus temperature.

As explained earlier, the temperature corresponding to these abrupt falls in modulus exactly coincide with the Curie temperature transition

6. Conclusions:

Finally, we have addressed some relevant findings on the importance NiMgCuZn ferrites that longitudinal modulus can be used as a powerful tool to examine the phase transitions in solids. Studies reveals that the formation of single phase spinel structure of all the samples. The lattice constant (a) unitcell volume (V) were estimated.

microstructural studies with the help of scanning electron microscopy (SEM) revealed uniform grain structure

The elastic behaviour of these ferrites revealed that there are abrupt falls at Curie Temperatures where these ferrite samples transform from ferromagnetic phase to paramagnetic phase.

Acknowledgments

This work was financially supported by Defence Research and Development Organization (DRDO), under the grants ERIP/ER/0103301/M/01, New Delhi, India. The author is thankful to the authorities of Sri Krishnadevaraya University, Anantapur for providing the facilities.

Author contribution statement:

I am the corresponding author. This work is the part of research work carried out at S.K.University, Anantapur, India. In order to develop a soft ferrite useful for micro inductors, Studies on different properties were carried out, One of these ferrites composition showed stress insensitivity after doping.

Table.1. Basic data of quartz transducers employed in the present investigation.

Type of quartz transducer	No.	Mass $m \times 10^3$ (kg)	Natural frequency f_c (kHz)
X-cut	1	0.8144	130.253
	2	0.7274	142.150
	3	0.6299	144.460
	4	0.5350	147.844

Table.2 . Elastic compliance S_{11} of sodium chloride at different temperatures.

f_c of quartz transducer employed 144.460 kHz.

T (°C)	L x 10 ² (m)	$\rho \times 10^2$ (Kg m ⁻³)	f_s (kHz)	$S_{11} \times 10^{12}$	
				Present Study	Hunter and Siegel 75
30	1.4724	2.1685	152.471	22.87	22.87
60	1.4744	2.1604	150.395	23.54	23.61
80	1.4768	2.1550	148.495	24.12	24.10
100	1.4792	2.1494	147.219	24.53	24.53
120	1.4816	2.1438	145.771	25.00	25.00
170	1.4856	2.1295	141.829	26.44	26.43
225	1.4911	2.1135	137.589	28.10	28.10
270	1.4947	2.1000	134.400	29.50	29.51
330	1.4983	2.0817	129.409	31.94	31.92

Table 3. Variation of longitudinal modulus with composition in NiMgCuZnFe₂O₄ system.

S.No	Composition	Longitudinal Modulus (L)	Curie point T_c (°C) GPa	Temperature at which peaks are Observed (°C)
Series-I				
1	Ni _{0.5} Mg _{0.5} Cu _{0.1} Zn _{0.3} Fe ₂ O ₄	157.1	230	210
2	Ni _{0.1} Mg _{0.5} Cu _{0.1} Zn _{0.3} Fe ₂ O ₄	155.7	270	270
3	Ni _{0.1} Mg _{0.3} Cu _{0.1} Zn _{0.3} Fe ₂ O ₄	162.9	290	290
4	Ni _{0.2} Mg _{0.3} Cu _{0.1} Zn _{0.3} Fe ₂ O ₄	179.3	300	300
Series-II				
1	Ni _{0.2} Mg _{0.3} Cu _{0.1} Zn _{0.3} Fe ₂ O ₄	151.2	210	215
2	Ni _{0.1} Mg _{0.3} Cu _{0.1} Zn _{0.3} Fe ₂ O ₄	151.8	280	280
3	Ni _{0.1} Mg _{0.3} Cu _{0.1} Zn _{0.3} Fe ₂ O ₄	179.3	300	300
Series-III				
1	Ni _{0.15} Mg _{0.3} Cu _{0.05} Zn _{0.3} Fe ₂ O ₄	170.8	190	190
2	Ni _{0.15} Mg _{0.1} Cu _{0.05} Zn _{0.3} Fe ₂ O ₄	159.9	220	220
3	Ni _{0.15} Mg _{0.1} Cu _{0.05} Zn _{0.3} Fe ₂ O ₄	148.6	290	290

Table 4. Lattice parameter and density values of all the three series of NiMgCuZn ferrites at room temperature.

S.No	Sample Parameter	Lattice kg.m^{-3}	Density
1	$\text{Ni}_{0.0}\text{Mg}_{0.6}\text{Cu}_{0.1}\text{Zn}_{0.3}\text{Fe}_2\text{O}_4$	8.374	4.267
2	$\text{Ni}_{0.1}\text{Mg}_{0.5}\text{Cu}_{0.1}\text{Zn}_{0.3}\text{Fe}_2\text{O}_4$	8.274	4.442
3	$\text{Ni}_{0.2}\text{Mg}_{0.4}\text{Cu}_{0.1}\text{Zn}_{0.3}\text{Fe}_2\text{O}_4$	8.255	4.665
4	$\text{Ni}_{0.0}\text{Mg}_{0.6}\text{Cu}_{0.1}\text{Zn}_{0.3}\text{Fe}_2\text{O}_4$	8.234	5.321
5	$\text{Ni}_{0.3}\text{Mg}_{0.1}\text{Cu}_{0.1}\text{Zn}_{0.5}\text{Fe}_2\text{O}_4$	8.260	4.498
6	$\text{Ni}_{0.3}\text{Mg}_{0.2}\text{Cu}_{0.1}\text{Zn}_{0.4}\text{Fe}_2\text{O}_4$	8.252	4.534
7	$\text{Ni}_{0.3}\text{Mg}_{0.1}\text{Cu}_{0.1}\text{Zn}_{0.5}\text{Fe}_2\text{O}_4$	8.234	5.321
8	$\text{Ni}_{0.35}\text{Mg}_{0.0}\text{Cu}_{0.05}\text{Zn}_{0.6}\text{Fe}_2\text{O}_4$	8.314	5.568
9	$\text{Ni}_{0.35}\text{Mg}_{0.1}\text{Cu}_{0.05}\text{Zn}_{0.5}\text{Fe}_2\text{O}_4$	8.255	4.742
10	$\text{Ni}_{0.35}\text{Mg}_{0.2}\text{Cu}_{0.05}\text{Zn}_{0.4}\text{Fe}_2\text{O}_4$	8.247	4.459

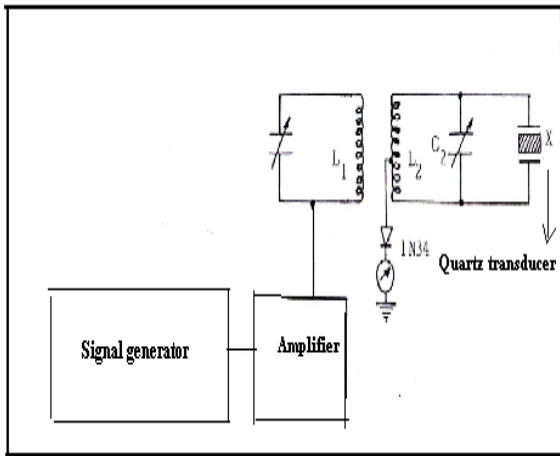


Fig.1. Block Diagram of Composite Oscillator.

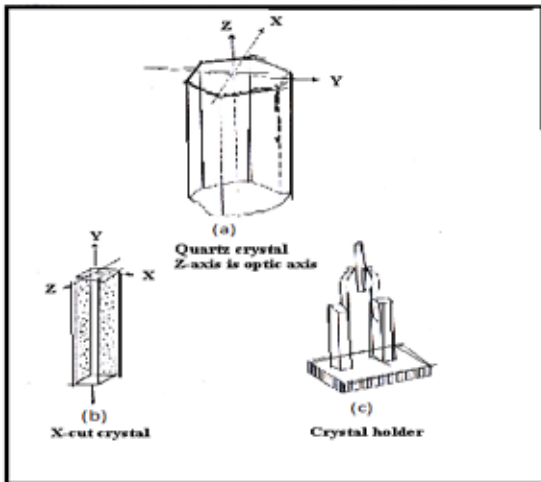
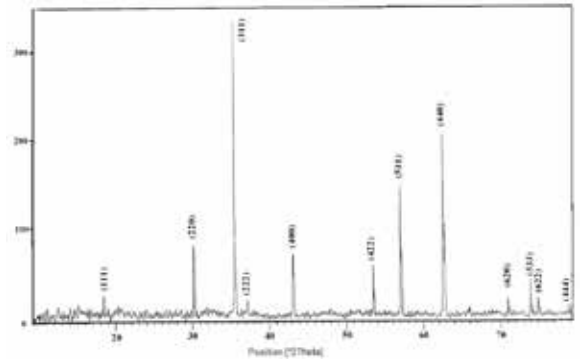
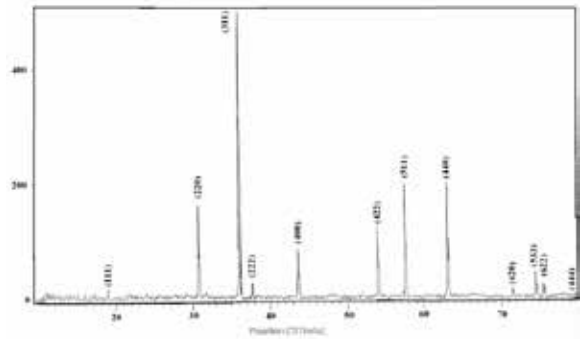


Fig.2 Electrode arrangement and mounting of X- Cut quartz crystal.

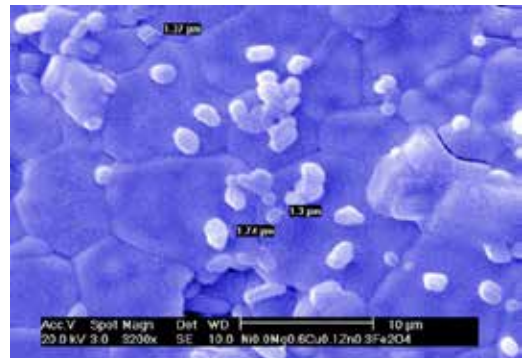


(a)

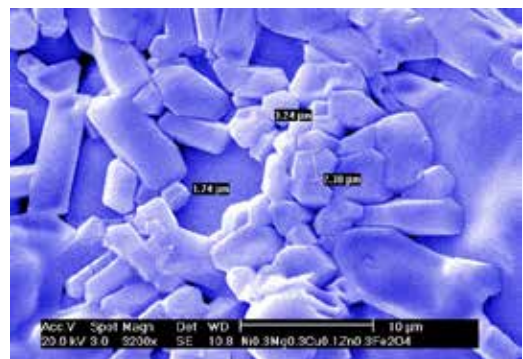


(b)

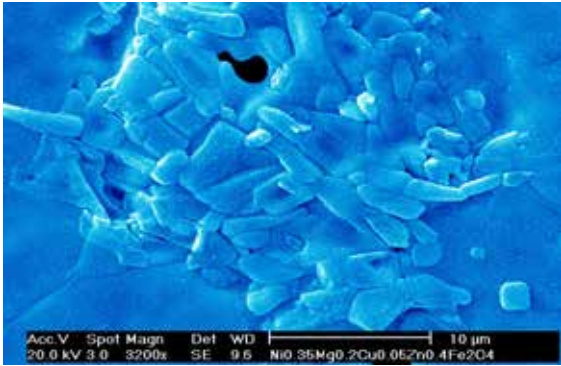
Fig.3. X-ray diffractograms for (a) Series 1, X = 0.1 (b) Series 2, X = 0.3



(a)



(b)



(c)
Fig.4 SEM patterns for (a) Series 1 (b) Series 2 and (c) Series 3.

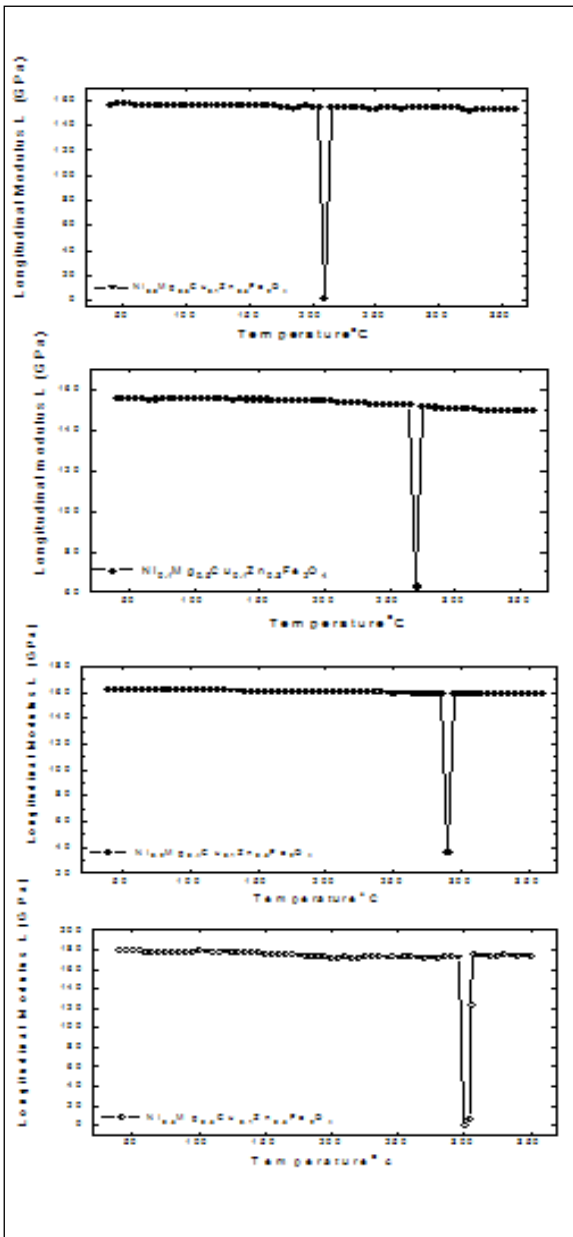


Fig.5 Variation of longitudinal modulus with temperature for series I

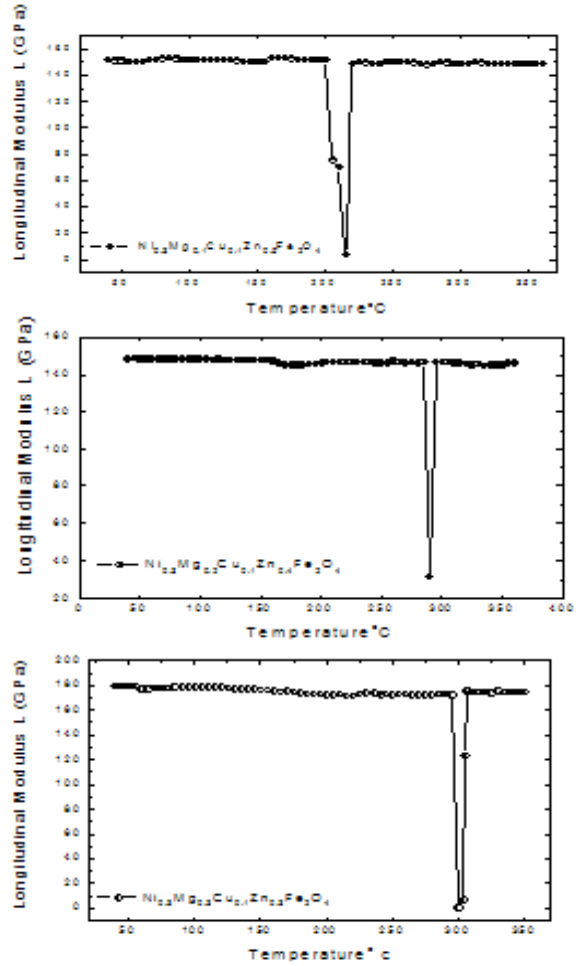


Fig.6 Variation of longitudinal modulus with temperature for series II

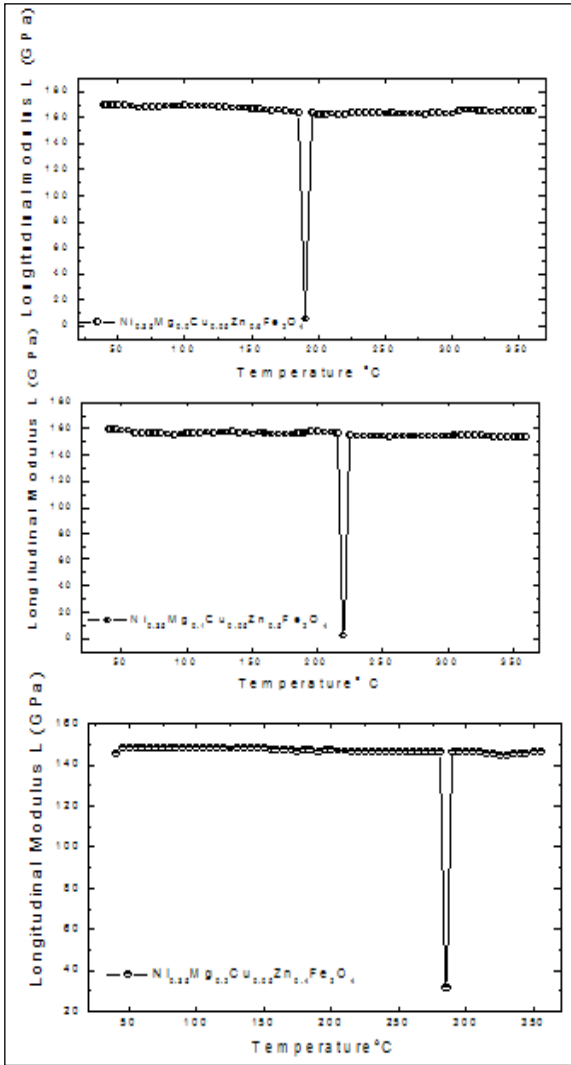


Fig.7 Variation of longitudinal modulus with temperature for series III

REFERENCE

- [1]. Weil, L., Ann. Inst. Fourier, 2 "Variation du module d'Young d'un ferrite avec | la Densite" pp.207 -213 (1950). [2]. Van der Burgt.C. M., Electron. Technl., 'Piezomagnetic ferrites' 37 pp.330- 341 | (1960). [3]. Fine. M. E. and Kenney.N.T., Phys. Rev., Moduli and Internal Friction of | Magnetite as Affected by the Low-Temperature Transformation 94 pp.1573- | 1576, (1954). [4]. McSkimin H. J., Williams A. J. and Bozorth R. M., Phys. Rev., 95 pp.616 (1954). [5]. Fine. M. E. and Kenney. N.T. Phys. Rev., Low-Temperature Acoustic Relaxation | in Ni-Fe Ferrites 96 pp.1487-1488 (1954). [6]. Gibbons. D. F., J. Appl. Phys., 28 pp.97 (1957). [7]. Van der Burgt C. M., Philips Res. Rep., 12 pp.97 (1957). [8]. Goryaga A. N., Phys. Met. and Metall., (GB) 12 pp.142 (1962). [9]. Kimura. Y. and Kashihabara S., Mem. Def. Acad., (Japan) 2 pp.51 (1963). [10]. Kuznetsov V. N., Phys. Met. and Metall., (GB) 15, pp.3 (1964). [11]. Kuznetsov.V. N., Phys. Met. and Metall., (GB) 19 pp.1 (1965). [12]. Novikov E. N., Stalmashenko and Botakii A. A., Sov. Phys. J., (USA), 11 | pp.127 (1967). [13]. Belov K. P., Sov. Phys. JETP (USA), 57 pp.1124 (1969). [14]. Terstegge H., Z. Angew. Phys., (Germany) 30 pp.103 (1970). [15]. Haudek. H. and Linke.D., Z. Angew. Phys., (Germany) 30 pp.129 (1970). [16]. Seshagiri Rao T., Revathi. B. and Purnanandam. M., Ind. J. Pure and Appl., | Phys., 9 pp.797 (1971). [17]. Revathi. B. and Rao. T. S., Ind. J. Pure and Appl. Phys., 7 pp.654 (1969). [18]. Murthy. S. R. and Rao. T. S., J. Acoust. Soc. India., 3 pp.9 (1975). [19]. [20]. Revathi. B. and Rao T. S., J. Less. Comm. Metals, 34 "Elastic behaviour | of mixed cobalt-zinc ferrites" pp.91-96 (1974). [21]. Seshagiri Rao T and Revathi. B. Ind. J. Pure and Appl. Phys., 10 pp.217 (1972). [22]. Wachtman Jr, J. B., Lam Jr D. G., and Apstein G. S., Phys. Rev., 122 "Exponential | Temperature Dependence of Young's Modulus for Several Oxides" pp.1754- | 1759 (1961). [23]. Kaczowski Z., Sov. Phys. Acoust., 14 "Temperature dependence of | piezomagnetic coefficients of ferrites", pp.183-190 (1968). [24]. Reddy B. P. N. and Reddy P. N., Brit. J. Appl. Phys., 1 "A note on the | elastic moduli of ferrites at low temperatures" pp.1213-1214 (1968). [25]. Reddy P. V, Reddy M. P., Muley Y. N., Reddy K. B. and Ramana. Y.V. J. Mater. Sci. Letts., 7 pp.1243 (1988). [26]. Reddy P.V., Phys. Stat. Solidi., (Germany) 10 pp.607 (1988). [27]. Tanaka T., Jap. J. Appl. Phys., (Japan) 14 "Young's and Shear Moduli, | Hardness and Bending Strength of Polycrystalline Mn-Zn Ferrites" pp.1897- | 1901 (1975). [28]. Murthy S. R. and Rao T. S., J. Mater. Sci. Letts., 2 "ΔE Effect of | polycrystalline Ni- Zn ferrites" pp.625-628 (1983). [29]. Murthy S. R., Reddy P.V and Rao T. S. J. Mater. Sci. Letts., 3 "Elastic | behaviour of mixed Manganese -magnesium ferrites" pp.647-650 (1984). [30]. Murthy S. R. and Rao T. S., Phys. Stat. Solidi., (Germany) 88 "Elastic | behaviour of mixed Li-M ferrites" pp.239-243 (1985). [31]. Murthy S. R., Chary M. L. and Rao C. N. "Proc of 5th International. | Conference on Ferrites", Bombay, India pp.315 (1989). [32]. Kawai Y. and Ogawa T., Phys. Stat. Solidi., (Germany) 76 " E effect of a Mn | ferrite single crystal at temperatures between 150 and 300 K" pp.375-381 | (1983). [33]. Gendelev S. Sh., Cruseba E.K. Saenko V., I. B. and Titov S. V. Sov. | Phys. Crystallogr., (USA) 30 (1985) pp.431. [34]. Komalamba B., Sivakumar K. V. and Murthy. V. R. K. Phys. Stat. Solidi., (a) 161 | "Effect of Magnetic Field on the Temperature Variation of Internal Friction Loss of Mn-Zn Spinel Ferrites in the Manganese-Rich Region" pp.53-58 (1997). [35]. Belov K. B., Kadamtseba A. M., Krynetskii I. B., Kovtun N. M., Mila V. N. | and Khokhlov V. A. Sov. Phys. Solid State., (USA) 17 pp. 416 (1975). [36]. Ryabinkin L. and Kapitonov N., Bull. Acad. Sci. (USSR), Phys. Ser., (USA) 34 | pp.975 (1970). [37]. Hoffmann P. O., J. Am. Ceram. Soc., 40 "Magnetic and Magnetostrictive | Properties of Magnesium-Nickel Ferrites" pp.250-252 (1957). [38]. Marx J., Rev. Sci. Instrum., 22 "Use of the Piezoelectric Gauge for | Internal Friction Measurements" pp.503-509 (1951). [39]. Kester E., Rabbe U., Presmanes L., Tailhades Ph. and Arnold W., J. Phys. and Chem. | Solids., 61 "Measurement of Young's modulus of nanocrystalline ferrites with | spinel structures by atomic force acoustic microscopy" pp.1275-1284 (2000). [40]. Kawai Y., Brabers V. A. M. and Simsa. Z. J. Magn. Magn. Mater., 157/158 | "Elastic and magneto-elastic properties of Mn-rich manganese ferrites" pp.537- | 538 (1996). [41]. Ravinder D., Mater. Letts., 47 "Effect of sintering temperature on | elastic behaviour of mixed Li-Cd ferrites" pp.35-39 (2001). [42]. Ravinder D., Balachander L. and Venudhar Y. C., Mater. Letts., 49 | "Elastic behaviour of manganese substituted lithium ferrites" pp.205- 208 (2001). [43]. Venudhar Y. C. and Satya mohan K., Mater. Letts., 55 "Elastic behaviour | of lithium-cobalt mixed ferrites" pp.196-199 (2002). [44]. Kawai Y. and Ogawa T., J. Phys. Soc. Japan., 45 Anelasticity in an Mn- | Ferrite Single Crystal pp.815-821 (1978). [45]. Ramamanoah Reddy N., Rajagopal E., Sivakumar K. V. Patankar K. K. and | Murthy V. R. K. Journal of Electroceramics., 11 "Effect of temperature on | the elastic and anelastic behaviour of magneto-ferroelectric composites | Ba_{0.8}Pb_{0.2}TiO₃ + Ni_{0.93}Co_{0.02}Mn_{0.05}Fe_{1.95}O₄ - in the ferroelectric rich region," | pp.167-172 (2003). [46]. Schwarz. R. B., Rev. Sci. Instrum., "Simple system using one-crystal component | oscillator for internal friction and modulus measurements," 48 pp.111-115 | (1977). [47]. Venugopal Reddy P., Muly V. N., Bhupal Reddy K. and Ramana Y. V. Solid. | State Comm., 6 "A study of elastic behaviour and internal friction of aluminium | substituted magnesium-copper ferrites" pp.449-452 (1998). [48]. Reddy B. P. N. and Reddy P. J., Phil. Mag., 30 "Elastic moduli of some ferrites | at low temperatures" pp.557-563 (1974). [49]. Gibbons D. F., J. Appl. Phys., 28 "Acoustic Relaxations in Ferrite Single Crystals | pp.810-814 (1957). [50]. Birch F., J. Geophys. Res., 66 "The Velocity of Compressional Waves in Rocks to | 10 ilobars, Part 2" pp.2199-2224 (1961). [51]. Birch F., J. Geophys. Res., 4 pp.295-311 (1964). [52]. Simmons G., J. Geophys. Res., 69 "Velocity of Compressional Waves in | Various Minerals at Pressures to 10 Kilobars" pp.1117-1121 (1964). [53]. Simmons G., J. Geophys. Res., 69 "Velocity of Shear Waves in Rocks to | 10 Kilobars, Part 1" pp.1123-1130 (1964). [54]. Anderson O. L., "Physical Acoustics, Principles and Methods", | IIB, | Academic press, New York pp.45 (1965). [55]. Ravinder D. and Vijaya Bhasker Reddy P., Mater. Letts., 57 "Composition of | room temperature elastic properties of mixed Li-Cu ferrites" pp.4575-4577 | (2003). [56]. Ravinder D. and Ravi Kumar B., Mater. Letts., 57 "A study on elastic behaviour | of rare earth substituted Mn-Zn ferrites" pp.4471-4473 (2003). [57]. Ravinder D., Mater. Letts., 45 "Elastic behaviour of lithium ferrites" pp.125- | 127 (2000). [58]. Ravinder D., Vijaya kumar K. and Boyanov B. S., Mater. Letts., 38 | "Elastic behaviour of Cu-Zn ferrites" pp.22-27 (1999). [59]. Ravinder D. and Alivelumanga T., Mater. Letts., 37 "Composition dependence | of elastic behaviour of mixed manganese-zinc ferrites" pp.51-56 (1998). [60]. Nitarand Kumar, Y. Purushotham, P. Venugopal, Z. H. Zaidi and Pran Kishan. J. | Magn. Magn. Mater., 192 "Elastic behaviour of Zn-substituted LiMg and | LiMgTi ferrites" pp.116-120 (1999). [61]. Abd El-Ati M. I. and Tawfik A., J. Ther. Anal. and Calor., 37 "Mechanical | and electrical properties of Ni_{0.65}Zn_{0.35}Cu_xFe_{2-x}O₄ Ferrite" pp.2465 - | 2471 (1991). [62]. Voigt W., "Lehrbuch der Kristalphysik," | Leipzig pp.962 (1928). [63]. Tutton A. E. H., "Crystallography and Practical Crystal Measurements", | I (1922). [64]. Bridgman P. W., Proc. Amer. Acad., 60 pp.305 (1925). [65]. Mandell W., Proc. Roy. Soc., A116 pp.626 (1927). [66]. Hanson A. W., Phys. Rev., 45 "Elastic Behavior and Elastic Constants of | Zinc Single Crystals" pp.324-331 (1934). [67]. Hinz. H., Zeit. F. Physik., 111 "Elastische Deformationen am Seignettesalz" | pp.617-632 (1939). [68]. Swift I. H. and Tyndall. S. P. T. Phys. Rev., 61 "Elasticity and Creep of Pb | Single Crystals" pp.359-364 (1942). [69]. Wright. S. J., Proc. Roy. Soc., (London) A126 pp.613 (1930). [70]. Davies. R. M., Phil. Mag., 16 "On the determination of some of the elastic | Constants of Rochelle Salt by a dynamical method" pp.97-124 (1933). [71]. Goens E., Ann. der Physik., 17 pp.233 (1933). [72]. Mason W. P., Phys. Rev., 55 "Dynamic measurement of the properties | of rochelle salt," pp.775-789 (1939). [73]. Hunter L. and Siegel S., Phys. Rev., 61 "The Variation with Temperature of the | Principal Elastic Moduli of NaCl near the Melting Point" pp.84-90 (1942). [74]. Atanasoff J. V. and Hart P. J., Phys. Rev., 59 "Dynamic Determination of the | Elastic Constants and Their Temperature Coefficients for Quartz" pp.85-96 | (1941). [75]. Bhagavantam S. and Suryanarayana D., Proc. Ind. Acad. Sci., A 20 pp.304 (1944). [76]. Ide. J. M., Rev. Sci. Instru., 6 "Some Dynamic Methods for Determination | of Young's Modulus" pp.296-298 (1935). [77]. Bordoni. P. G., J. Acoust. Soc. Amer., 26 Elastic and Anelastic Behavior of | Some Metals at very Low Temperatures pp.495-502 (1954). [78]. Fine M. E., ATSM Bull., 181 pp.20 (1952). [79]. Wegel R. L. and Walther H., Physics., 6 Internal dissipation in solids for | small cyclic strains pp.141-157 (1935). [80]. Forster F., Z. Metallkd., 29 pp.109-115 (1937) [81]. Forster F. and Koster W., Z. Metallkd., 29 pp.116 (1937). [82]. Spinner. S., J. Amer. Chem. Soc., 37 Elastic Moduli of Glasses by a | Dynamic Method. pp.229-234 (1915). [83]. Bradfield G., Brit. J. Appl. Phys., 11 "Dynamic measurement of elasticity | using resonance methods" pp.478-480 (1960). [84]. Van der Burgt C. M., Philips Res. Rep., 8 pp.91 (1953). [85]. Curien H, Acta Cryst., 5 "Diffusion thermique des rayons X par des | monocristaux de fer- et dynamique du réseau cubique centré" pp.393 (1952). [86]. Jacobsen E. H., Phys. Rev., 97 "Elastic Spectrum of Copper from Temperature- | Diffuse Scattering of X-Rays" pp.654-659 (1955). [87]. Johnson R. E., Phys. Rev., 94 "Elastic Spectrum of Zinc from the | Temperature Scattering of X-Rays" pp.851-855 (1954). [88]. Gunther, Z. Kristallogr., 103 (1941). [89]. Wooster W. A. and Ramachandran. G. N., Acta Cryst., 335 "Determination of | Elastic constants of crystals from diffuse reflexions of X-rays. II. Application to | some cubic crystals" pp.431-440 (1951). [90]. Bergmann L. and Schaefer, Litz. Ber. Berliner. Akad., pp.132 (1934). [91]. Bolef D. I. and Menes M., J. Appl. Phys., 31 pp.245 (1936). [92]. Hiedemann. E., Ultrasonics., (1938). [93]. Bhagavantam S. and Ramachandra Rao B. Nature., 162 "Elastic Constants of | Alum Determined by a New Ultrasonic Method" pp.818-819 (1948). [94]. Bhagavantam S. and Bhimasenchar B., Prof. Ind. Acad. Sci., A 20 pp.298 (1944). [95]. Bhagavantam S. and Bhimasenchar B., Proc. Roy. Soc., A 187 pp.381 (1946). [96]. Huntington. H. B., Phys. Rev., 72 "Ultrasonic Measurements on Single | Crystals" pp.321-331 (1947). [97]. Arenberg D. L., J. Appl. Phys., 21 "Determination of Elastic Constants in | Single Crystals with Especial Reference to Silver Chloride" pp.941-942 (1950). [98]. McSkimin H. J. Appl. Phys. 24, "Measurement of Elastic Constants at Low | Temperatures by Means of Ultrasonic Waves-Data for Silicon and Germanium Single Crystals, and for Fused Silicon" pp.988-998 (1953). [99]. Bacon R. and Smith. C. S., Acta metallurgical., 4 "Single crystal elastic constant | of silver and silver alloys" pp.337-341 (1956). [100]. Musgrave. M. J. P., Proc. Met., 4 (1956) pp.337. [101]. Galt J. K., Proc. Phys. Soc., (London) B68 pp.81 (1955). [102]. Overtone W. C., Phys. Rev., 73 "Mechanical Properties of NaCl, KBr, | KCl" pp.1460-1462 (1948). [103]. Featherston F. H. and Neighbours. J. R. J. Chem. Phys., 18 "the | vibrational frequencies of ethylene" pp.113-122 (1950). [104]. Featherston. F.H. and J.R. Neighbours., Phys. Rev., 130 "Elastic Constants | of Tantalum, Tungsten, and Molybdenum" pp.1324-1333. (1963). [105]. Lazarus.D., Phys. Rev., 76 The Variation of the Adiabatic Elastic Constants | of KCl, NaCl, CuZn, Cu, and Al with Pressure to 10,000 Bars pp.545-553 (1949). [106]. H. J. McSkimin and P. Andreatch "Elastic Moduli of Germanium Versus | Hydrostatic Pressure at 25.0°C and -195.8°C" J. Appl. Phys. 34, pp.651-656 | (1963) [107]. Mc Skimin. H. J., "Physics of Solids at High Pressures" (Academic Press | Inc., N.Y., pp.510 (1965). [108]. H. J. McSkimin. J. Acoust. Soc. Amer., 22 " Ultrasonic Measurement Techniques | Applicable to Small Solid Specimens" pp.413 (1950). [109]. Papadakis E.P., J. Acoust. Soc. Am. 42, "Ultrasonic Phase Velocity by the | Pulse-Echo-Overlap Method Incorporating Diffraction Phase Corrections" pp. | 1045-1051 (1967) [110]. Balamuth. L., Phys. Rev., 45 "A New Method for Measuring Elastic | Moduli and the Variation with Temperature of the Principal Young's | Modulus of Rocksalt Between 78°K and 273°K" pp.715-720 (1934). [111]. Rose. F. C., Phys. Rev., 49 "The Variation of the Adiabatic Elastic Moduli of | Rocksalt with Temperature Between 80°K and 270°K" pp.50-54 (1936). [112]. Van Dyke K. S., Proc. I.R.E., 11 pp.742 (1928). [113]. Kincoid. J. F. and Eyring.H., J. Chem. Phys., 6, "A partition function for liquid | Mercury" pp.587-597 (1937). [114]. Kincoid. J. F. and Eyring. H., J. Chem. Phys., 6, "Free volumes and free angle | ratios of molecules in liquids" pp.620-630 (1938). [115]. Koster W. and Bangert I., Z. Metallk., 42 pp.391 (1951). [116]. Huntington. H. B. "The Elastic Constants of Crystals" Academic press, | NewYork, pp.127 (1958). |